Numerical approach of cyclic behavior of 316LN stainless steel based on a polycrystal modeling including strain gradients.

Julien Schwartz, Olivier Fandeur, Colette Rey

Numerical approach of cyclic behavior of 316LN stainless steel based on a polycrystal modeling including strain gradients.

JulienSchwartz[a,b], Olivier Fandeur[c], Colette Rey[a]

[a]Laboratoire Mécanique Sols, Structures et Matériaux, CNRS, UMR 8579, Ecole Centrale Paris, grande voie des vignes, F-92295 Chatenay-Malabry, France.
[b] Electricité de France, Département MMC R&D, F-77818Moret-sur-Loing, France.
[c]CEA, DEN, DM2S, SEMT, LM2S, F-91191 Gif-sur-Yvette, France.

Corresponding author: C. Rey,colette.rey@ecp.fr

Abstract
Anon-local polycrystal approach,taking into account strain gradients, isproposedto simulate the 316LN stainless steel fatigue life curve in the hardening stage.Material parameters identification is performed on tensile curves corresponding to several 316LN polycrystalspresenting different grain sizes. Applied to an actual 3D aggregate of 316LN stainless steel of 1,200 grains, this modelleads to an accurate prediction of cyclic curves.Geometrical Necessary Dislocation densities related to the computed strain gradient are added to the micro-plasticity laws. Compared to standard models, this model predicts a decrease of the local stresses as well as a grain size effect.

Keywords: low cycle fatigue; non-local polycrystalline model;grain size, austenitic stainless steel.

1. Introduction

Implemented in finite element codes, standard polycrystal models (based on dislocation density evolution), gave a first hint of grain size effects through the shear stresses heterogeneities [1]. If such models gave a first order description of plastic deformation related to dislocation motion, they could not describe the grain size effect on the mechanical behaviour evolutionof polycrystals. By introducing a mechanical interaction between mobile dislocations and grain boundaries, some authors,such as Ma et al [2], showed that standard polycrystal models are sensitive to grain geometry. Despitethese recent improvements, standard polycrystalmodelsstill could not predict,both tensile and fatigue behaviours, with the same set of material parameters. The aim of this paper is to propose a numerical non-local polycrystal model able to directly predictthe fatigue behaviour from tensile tests and its evolution with grain size by introducing Geometrically Necessary Dislocation (GND) densities into the constitutive laws of a polycrystal standard model.
For the last 15 years, different formulations of constitutive lawshave been proposed, to describe the microstructure evolution in the grains of polycrystals submitted to plastic deformation. Related to the grain size, such formulations required constitutive laws introducing the strain gradient evolution in the grains. These works werereviewed by McDowell [3, 4],who analysed the different tools for computation modeling and for simulation bound to inelastic deformation phenomena,from atomistic to structural length scales.
Except someworks based on generalized continuous-medium[5, 6, 7] and on Cosserat type coupled stress theories [8, 9, 10, 11], most papersdealt with the strain gradient theories. Grain size effect on macroscopicalas well as on microscopicalmechanical behaviour,was based on the concept of Geometrically Necessary Dislocations introduced by Nye [12]and Ashby [13] .As shown by Eshelby [14] and Kröner [15] , the GNDs are required to accommodate the elastic and plastic incompatibilities between grains. Ensuring compatibilities between grains,the Finite Element techniquegives a good approximation of local strain and stress fields at grain boundaries, but cannot take into account the grain size effect on mechanical properties. In polycrystals, local stress and strain fieldsare generally heterogeneousand presentstrain gradientsat the vicinityof grain boundaries and within grains. The GNDsare bound to such strain gradients.
Several non-local rate dependent crystallographic formulations for finite strainswere proposed by Beaudoin et al [16],Acharya et al [17, 18, 19, 20, 21],Meissonnier et al [22],Raabe et al [23] and Evers

et al [24].Most of them were based on the framework of finite deformations, as defined by Asaro et al [25, 26, 27] and Peirce et al [28,29]. These non-local formulations, introduced GNDs densities into the constitutive laws. Relations between the elastic or plastic transformation field gradientsand the specific burgers vector of the GNDs were proposed by Acharya et al [18],Gurtin [30, 31, 32] and Cermelli and Gurtin [33].They showed that the transformation gradient is related to the GND density tensor of Nye [12], Ashby [13], Eshelby [14] and Kröner [15]. Suchnon-local models found several successful applications formechanical behaviour of polycrystals, such as: hardening phenomena [19],grain size effect [17, 34],hardening due to particles [35],texture [36] and local mechanical fields predictions [2].

Macroscopical models of fatigue based on phenomenological equations [37, 38, 39], gave a good prediction of the macroscopic behaviour of materials submitted to low cycle fatigue. But, compared to a polycrystal approach based on dislocation micro-plasticity laws, they could not describe accurately the grain size effect and the micro-behaviour such as local fields. The mechanical behaviour being mainly linked to the dislocation microstructure evolutions (which are different for the tensile and for cyclic tests) we use constitutive laws function of dislocation densities. The GNDs (deduced from strain gradient computations) are introduced to relax stresses due to local incompatibilities and to describe more accurately the dislocation pattern evolution at the end of hardening stage. At the end of the hardening stage fatigue, the microstructure is composed of veins and channels which correspond to Persistent Slip Bands (PSBs) observed at the surface of the samples. Recently, the polycrystal modelling was applied to fatigue. Schwartz et al [40] showed that such approach gave a good description of PSBs initiation in the hardening stage of low cycle fatigue. Le Pécheur et al [41] successfully simulated the beginning of the stabilized stress-strain curves and compared different local micro-damage criteria. Li et al [42] proposed an accurate description of the softening stage and the associated local stress and strain fields, by assuming that the involved polycrystal was a two-phase material (veins and channels) which obeys the constitutive laws proposed by H. Mughrabi [43]. To point out the micro-mechanical consequences bound to GNDs introduction, we have chosen to suppress thekinematic law [44, 45] generally used to describe fatigue loading. Since the polycrystalmodeling must be intrinsic, dislocations micro-plasticity laws must be the same for any mechanical tests. To obtain some information on the validity of the constitutive laws taking into account GNDs, we have numerically tested these equations on tensile and low cycle fatigue loadings.In this first approach, the hardening stage is only studied.

In this paper, GNDsare introduced into a local polycrystalmodel [46, 47, 48].Implemented in a finite element code [49], our model isbased upon the continuum dislocation theory,in the framework of finite deformations. The internal mechanical fieldamplitudes and distributions within the grains are computed with the local and with our non-local approaches. Performed on 316LN stainless steel presenting 3 grain sizes,tensile tests give the input data for the parameter identifications of the local and non-local models (section 2). Our non-local polycrystalmodel is developed in section 3.In section 4, three sets of parameters areobtained for the local and non-local approaches (LA and NLA).The two models are applied to an actual316LN 3D aggregate submitted to tensile and fatigue tests. This aggregate is obtained by serial polishing and crystallographic orientations performed thanks to Electron Back Scattering Diffraction technique (EBSD). For both models, the obtained numerical tensile curves, the fatigue life curvesand the cyclic loops in the hardening stage are compared to experimental ones. In section 5, the distribution and amplitude of the internal stresses within the grains of the 3D aggregateare analysed for cyclic loadings. A discussion is given in section 6. A summary(section 7)ends the paper.

2. Material and experimental procedures

2.1 Material characteristics

Obtained by rolling followed by an austenitization and by a quenching,our 316LN steel was composed of a 99% face centered cubic austenitic phase and a1%body centered cubic residual δ ferritic phase.The 316LN compositionis given in table 1:

Elements	C	Mn	Si	P	S	Cr	Ni	Mo	N	Nb	Ti	Ta	Cu	B	Co	Fe

| Min. | - | 1,6 | - | - | - | 17,0 | 12,0 | 2,3 | 0,06 | - | **-** | **-** | **-** | **-** | **-** | |
| Max. | 0,03 | 2,0 | 0,5 | 0,025 | 0,1 | 18,0 | 12,5 | 2,7 | 0,08 | 0,01 | 0,01 | 0,15 | 0,3 | 0,001 | 0,05 | base |

Table1. Chemical composition of the 316LN stainless steel

The austenite and ferrite average grain sizes were 26µm and 10µm respectively. More than 30% of the austenitic grain boundaries corresponded to Σ_3 twins. The material presented a negligible texture.

To identify the material parameters of our non-local model, tensile tests were performed on different grain sizes. The 316LN presenting abnormal grain growth, only three different grain sizes were obtained by critical hardening technique: 26µm, 17µm and 13µm.

2.1.1   Tensile tests

The specimens were 2mm thick, with a 40mm gauge length. The tests were performed at room temperature with a 10^{-3} s^{-1} strain rate. The stress-strain curves at room temperature are given in Fig.1.
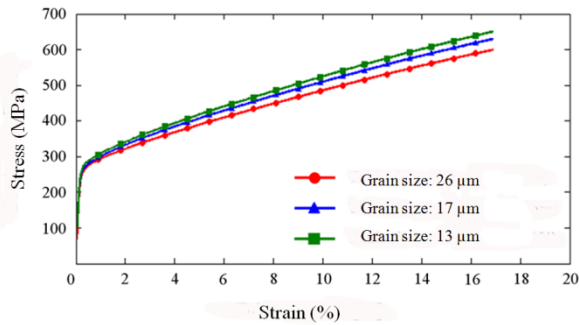

Fig.1. Tensile stress-strain curves for 316LN polycrystals presenting three grain sizes

The stress evolution versus the grain size is given in Fig. 2 and is compared to Kashyap et al [50],curves for a AISI 316L steel. The same order magnitude is obtained. The small differences observed for the two AISI316LN and AISI316L steels may be attributed to the different compositions of the two materials.Our 316LN obeys the Hall-Petch law given by Eq.1:
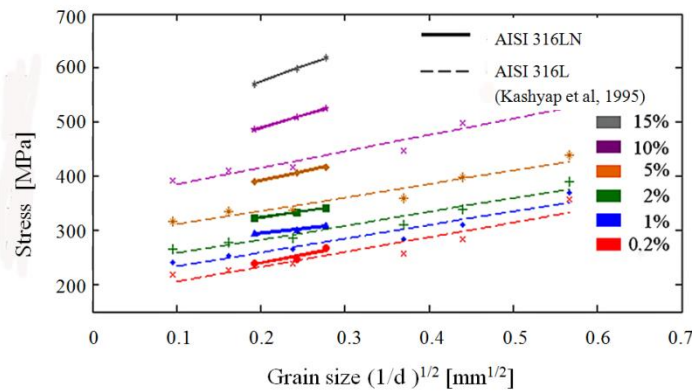
$$\sigma = \sigma_0 + k(1 / d)^{1/2} \ (1)$$

Fig.2. Experimental stress-grain size curves for several strain amplitudes. Comparison with the results of Kashyap et al [50].

2.1.2   Fatigue tests

Fatigue tests were performed on cylindrical specimens (8mm diameter and 6mm gauge length). The studied material corresponded to the 316LN with a 26 µm grain size.At room temperature,low cycles were performed on MTS 100kN, for two given strains ($\Delta\varepsilon/2 = 0.3\%$ and $\Delta\varepsilon/2 = 0.5\%$) at 10^{-3} s^{-}

[1].The results being close for the two strain amplitudes,only the $\Delta\varepsilon/2 = 0.5\%$ applied strain is presented in this paper.

The fatigue curves (Fig.3a) and the hysteresis loops (Fig.3b) are given for different fatigue life times: N_H corresponds to the cycle number at the end of the hardening stage, N_S to the end of the softening stage, $N_{1/2}$ to the half-life time and N_R to the rupture of the specimens.
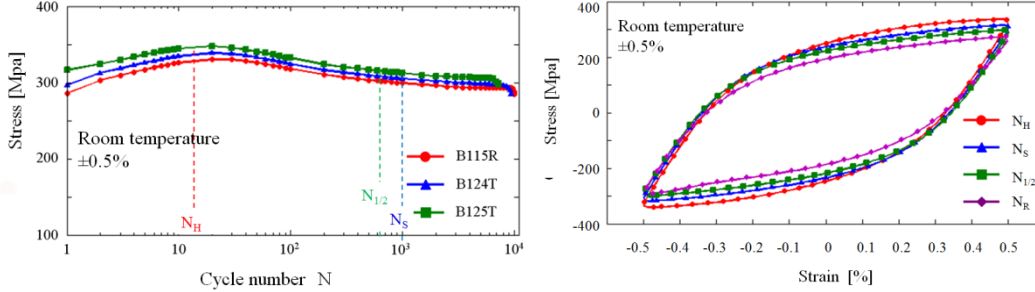

Fig.3. (a) Experimental fatigue curves for three 316LN identical specimens. (b) Cyclic stress-strain curves for different cycle numbers.

3. Polycrystalmodeling

This polycrystal plasticity model is an extension ofthe local approach proposed byErieau et al [46],Libert et al, [47],andCédat et al [48]. This model is developed in the framework of finite transformations (small elastic distortions but large lattice rotations), according to the scheme proposed by Asaro et al [25]and Peirce et al [28,29] for the case of single crystals. The approach was implemented in the Abaqus® finite element code, using aUser MATerial Subroutine.

3.1 Kinematic

The kinematic is based on the velocity gradient $\tilde{L}$ which is decomposed additively into an elastic part $\tilde{L}^e$ and a plastic part $\tilde{L}^p$ given by:

$$\tilde{L} = \tilde{L}^e + \tilde{L}^p \tag{2}$$

With $\tilde{L}^e = \dot{\tilde{F}}^e.\tilde{F}^e$ and $\tilde{L}^p = \dot{\tilde{F}}^p.\tilde{F}^p$. Where $\tilde{F}^e$ is the elastic part and $\tilde{F}^p$ the plastic part of the deformation gradient tensor $\tilde{F}$ given by:

$$\tilde{F} = \tilde{F}^e.\tilde{F}^p \tag{3}$$

In the following, we note: $(\tilde{A}.\tilde{B})_{ij} = A_{ik}B_{kj} \ and \ \tilde{A}:\tilde{B} = A_{ij}B_{ij}$

For small elastic strain $\tilde{\varepsilon}^e$ and large lattice rotations $\tilde{R}^e$ we have:

$$\tilde{F}^e \approx (1 + \tilde{\varepsilon}^e).\tilde{R}^e \tag{4}$$

The symmetric part of the velocity gradient is given by:

$$\tilde{D} = \tilde{D}^e + \tilde{D}^p \tag{5}$$

With: $$\tilde{D}^e \cong \dot{\tilde{\varepsilon}}^e \ and \ \tilde{D}^p = \sum_s \dot{\gamma}^s(\vec{g}^s \otimes_S \vec{n}^s) \tag{6}$$

The skew symmetric part (elastic and plastic parts) of the velocity gradient is given by:

$$\tilde{W} = \tilde{W}^e + \tilde{W}^p \tag{7}$$

With: $\tilde{W}^p = \sum_s \dot{\gamma}^s(\vec{g}^s \otimes_{AS} \vec{n}^s) \tag{8}$

4

and $\widetilde{W}^e = \dot{\widetilde{R}}^e . \widetilde{R}^e$ (9)

$\vec{g}^s$ and $\vec{n}^s$ are unit vectors representing respectively the slip direction and the normal to the slip plane of the slip system *(s)* in the current configuration. $\dot{\gamma}^s$ is the slip rate on the system (s) in the current configuration.

The Cauchy tensor rate $\widetilde{\sigma}$ does not satisfy the principle of objectivity, thus, as most authors, we introduce the Jaumann rate $\widetilde{\sigma}*$ given by:

$$\widetilde{\sigma}* = \sigma - \widetilde{W}^e . \widetilde{\sigma} + \widetilde{\sigma} . \widetilde{W}^e \text{ (10)}$$

At each time increment, the Jaumann rate tensor is bound to the elastic strain rate by the elastic moduli $\widetilde{\widetilde{C}}^e$ so that the Cauchy stress tensor rate can be expressed as:

$$\dot{\widetilde{\sigma}} = \widetilde{\widetilde{C}}^e : \widetilde{D}^e + \widetilde{W} . \widetilde{\sigma} - \widetilde{\sigma} . \widetilde{W} - \sum_s \dot{\gamma}^s \widetilde{R}^s \text{ (11)}$$

with: $\widetilde{R}^s = \widetilde{\widetilde{C}}^e : \widetilde{D}^s + \widetilde{W}^s . \widetilde{\sigma} - \widetilde{\sigma} . \widetilde{W}^s$ (12)

For infinitesimal strains, we assume that the Cauchy tensor $\widetilde{\sigma}$ is equal to the Kirchhoff stress tensor $\widetilde{\tau}$.

3.2 Non-local approach

Implemented in finite element code,polycrystal classical local approachescan predict heterogeneous strain stress and rotation fields within the grains, as well as sub-grain boundary formation. Piles up dislocation against the grain boundaries can be related to the observedstrain localization. Such heterogeneities generate strain incompatibilities and extra stresses.The non-local approach can compute the strain gradient between two adjacent points within the material.Deduced from the strain gradient,the extra GNDs reduce such incompatibilities.

The incompatibility of the plastic strain is measuredon the current configuration connected to the lattice configuration with an inverse elastic transformation tensor $\widetilde{F}^{e-1}$ by $curl(\widetilde{F}^{e-1})$.The ijcomponent is given by:

$$curl(F^{e-1})_{ij} = \varepsilon_{irs} \frac{\partial F_{js}^{e-1}}{\partial x_r} \text{ (13)}$$

where ε_{irs} is the alternating symbol. $curl(F^{e-1})_{ij}$ is thederivative of the elastic transformation tensor vector with respect to the vector position $\vec{x}(\vec{X},t)$ in the current configuration. The Burgers vector $\vec{b}^e$ of the GNDs in the current configuration corresponds to the closure failure associated to the continuous lattice circuit ∂S enclosing area S on a slipsystem with normal $\vec{r}$.

$$\vec{b}^e = \int_{\partial S} \widetilde{F}^{e-1} . d\vec{x} = \iint_S curl(\widetilde{F}^{e-1}) . \vec{r} ds \quad\quad (14)$$

The Burgers vector can be expressed as a function of the dislocation tensor $\widetilde{\alpha}$ defined by Nye [12]and Kröner [15]:

$$\vec{b}^e = \iint_S \widetilde{\alpha} . \vec{r} ds \quad\quad (15)$$

For each slip system (s),the identification of the 9 components of the tensor $\widetilde{\alpha}$ from experiments is not yet solved. Rather than introducing sucha dislocation tensor into the dislocation density evolution lawas Busso et al [35] and Ma et al [2],we usethe scheme proposed by Peirce et al [28,29]the incompatibility for slip system (s) is defined by onescalar λ^s via a third order tensor Λ. The relation between $\Lambda$and the Burgers vector of the GNDsin the current configuration is defined from the elastic transformation:

$$\vec{b}^e = \oint_{\partial S} \tilde{F}^{e-1} d\vec{x} = \iint_S \Lambda : \vec{r} dS = \iint_S \tilde{\alpha}.\vec{r} dS \quad (16)$$

With

$$\Lambda = \left(\frac{\partial \tilde{F}^{e-1}}{\partial \vec{x}}\right)_A \text{,or } \Lambda_{ijk} = F_{ij,k}^{e-1} - F_{ik,j}^{e-1} \quad (17)$$

According to Acharya et al [19], the third order tensor Λ represents the existence of a dislocation network threading the slip plane (s) with a unit normal $\vec{n}^s$.

The λ^s scalar is given by:

$$\lambda^s = \sqrt{(\Lambda : \vec{n}^s)(\Lambda : \vec{n}^s)} \quad (18)$$

The twelveλ^sscalars correspond to GND densities. They are determined at each computation time increment.

According to Needleman and Sevillano [51], the addition of new parameters bound to GNDsrequires a reformulation of the constitutive laws. Some authors, as Meissonnier et al [22],Busso et al [35], Evers et al [24] and Kadkhodapouret al [52] describedthe dislocation densitiesevolution by two equations: one for the statistically stored dislocations and a secondone for GNDs. In our non-local model, we introduce anextra parameter k_0, into the dislocation density evolution equations, via the definition of the mean free path of these GNDs [34]:

$$L_G^s = 1/k_0 \lambda^s \quad (19)$$

$k_0$is a material parameterwhich will be determined from our experimental tensile curves.

Acharyaet al [20] mentioned that this mean free path L_G^s is associated to the pile up on the grain boundaries and to the cell wall patterns. We have extended this mean free path to sub-grain boundaries due to deformation.

Using the continuum theory of dislocations, the statistically stored dislocation densities ρ^s and the GNDs λ^s on each slip system,are added and considered as internal variables of our model.

3.3   Single crystal plasticity laws

Our polycrystal model is developed for face centered cubic structure (fcc) as well as for bodycentered cubic structure(bcc) and for two-phase materials (which is the case of the austenitic stainless steel 316LN).

In this paper, the single crystal plasticity laws,as proposed by Tabourot et al [53]and issued from the works of Kocks et al [54], Kocks [55] and of Estrin and Mecking [56, 57],arehere modified to take into account the GNDs. They are applied to each grain assumed to have the behaviour of single crystals.

For fcc, the Schmidcriterion rules the activation of the 12 slip systems {110} <111>. For bccphase,the Schmidcriterion [58] is applied to the 24 slip systems {111} <110> and {111} <112>.

The criterion is given by:

$$|\tau^s| = \tau_c^s \quad (20)$$

where $\tau^s = (\tilde{\tau}.\vec{n}^s)\vec{g}^s$ is the reduced shear stress on the glide plane (s), as computed from Eq.8. τ_c^s is the critical shear stress.

The GNDs play the role of obstacles and are added to the statistically stored dislocation densities. For each time increment of the computation,we assume that the critical shear stress is given by:

$$\tau_c^s = \tau_0^s + \mu b \sqrt{\sum_{u=1,12} a^{su}(\rho^u + \lambda^u)} = \sum_u h^{su} \gamma^u \quad (21)$$

whereμ is the isotropic shear modulus, b the norm of the Burgers vector,τ_0^c the lattice friction stress, h^{su} the component of the hardening matrix. For the local approach $(\lambda^s = 0)$, the h^{su} matrix

6

describesan anisotropic hardening, which depends on the activated dislocations (i.e loading path). For the non-local approach $\left(\lambda^s \neq 0 \right)$, we assume that the h^{su} matrix describes both anisotropic and kinematic hardenings.

The critical shear stress, given by Eq.15 and Eq.16, is a function of the components a^{su} of the interaction matrix (forest hardening) between the systems (s) and (u). There is no evidence that the interactions between statistically stored dislocations with the forest obstacles are similar to interactions between these dislocations and the obstacles created by GNDs. But, in this first approach, we have used the same interaction matrix. Moreover, this matrix is an asymptoticvalue, when compared to the one proposed by Devincre et al [59], Queyreau et al [60] and Monnet et al [61]

For afcc single crystal, the 12x12 interaction matrix is composed of six different terms which are computed in section 4.The glide velocity $\dot{\gamma}^s$ is expressed with a classical viscoplastic potential based on the resolved shear stress and the critical shear stress for glide activating on system (s):

$$\dot{\gamma}^s = \dot{\gamma}_0 \left(\frac{|\tau^s|}{\tau_c^s} \right)^n sign(\tau^s) \ \ if \ \ |\tau^s| > \tau_c^s \tag{22}$$

$$\dot{\gamma}^s = 0 \ \ otherwise$$

Where $\dot{\gamma}_0$ is a reference shear rate and n isthe rate exponent.

The dislocation density evolution (Eq.18), is governed by a dislocation production term, based on Orowan relationship and is balanced by an annihilation dislocation term which takes into account the dynamic recovery during deformation.

$$\dot{\rho}^s = \frac{|\dot{\gamma}^s|}{b} \left[k_0 \lambda^s + \frac{\sqrt{\sum_{u \neq s} \rho^u}}{K} - 2 y_c \rho^s \right] \tag{23}$$

$2y_c$ is a material parameter related to an annihilation distance of dislocations. The first term corresponds to the inverse of the average mean free path L_G^s of GNDs, whereas the secondterm corresponds to the inverse of the average mean free path L_S^s of the statistically stored dislocations on the system (s). The third term corresponds to annihilation of dislocations. Material parametersk_0 and $K$are related to the two average mean free path on each slip system L_G^s and L_S^s. The evolution of L_S^s comes from the evolution of the dislocation densities on the other glide systems (u) which intersect the glide plane (s), through:

$$L_S^s = K / \sqrt{\sum_{u \neq s} \rho^u} \tag{24}$$

The equations are solved thanks to a scheme using the forward gradient approximation close to the scheme proposed by Peirce et al [28] and Teodosiu et al [62].

4. Aggregate, meshing, boundary conditions, model parameter identification

4.1 Aggregate

A representative volume of the material is required to analyse the effect of the actual material microstructure (containing a large amount of twin boundaries) on the local stress and strain fields. To avoid artefacts due to boundary conditions and free surfaces, a large aggregate volume is used. To obtain such a Representative Volume (RV) of the 316LN material, a 600 x 600 x150 µm³ aggregate was built,composed of 30 layers, each one corresponding to an Electron Back-Scattering Diffraction (EBSD) map extruded over 5µm (each layer thickness being then 5µm). The EBSD step analysis within a layer was 1µm. The mechanical technique consisted in successive polishings and in

crystallographic orientation measurements by EBSD. An experimental technique and specific software were developed for the reconstruction of the points meshing element, need large memory space and a large computing time. In this paper, all simulations are actually performed on a quarter of the aggregate (300 x300 x150 µm³) named AG2 (Fig.4c) containing 1,029 grains. The FE meshing is 4 x 4 x 5 µm³. For such an aggregate, the resolution is weak, compared to those obtained by Zaefferer et al [63], through Orientation Microscopy in a Focused Ion Beam-Scanning Electron Microscopy (FIB-SEM). However, our mechanical technique enables the investigation of a large amount of large grains. aggregate from the successive layers [49]. The 3D aggregate (AG1) contained 4,363 austenitic grains and 319 ferritic grains(Fig.4). Computations on such a large aggregate(Fig.4a and 4b), presenting small meshing (1 x 1 x 5 µm³) with eight Gauss
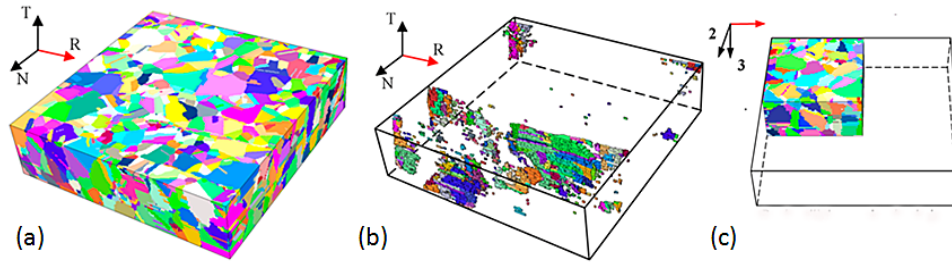

Fig.4. (a) 316LN 3dimensional aggregate (4,363 austenitic grains), (b) ferritic phase, (c) aggregate used for the simulations(1,029 austenitic grains).

4.2   Numerical scheme, meshing and boundary conditions

The polycrystal model is implemented in Abaqus software package®, using a User Subroutine (UMAT). The numerical scheme is an explicit forward gradient procedure which delivers a good accuracy as well as a high integration speed. Though this method presents the drawback to use very small time increments, it has the advantage to detect a progressive lattice reorientation (very small for fatigue tests) and the occurrence of new active glide systems. For such small time increments, our small elastic strain assumption is valid. Local stress and strain fields, dislocation densities, cumulated glide on the glide systems, total cumulated glide magnitude are respectively computed for each time increment, and for each Gauss point.In this first approach, the elastic transformation tensor is assumed equal to the lattice rotation $\tilde{F}^e \approx \tilde{R}^e$.

Via a post-treatment routine, the gradient of the lattice rotation is explicitly computed for each time increment.

As shown in Fig.5a,linear cubic elements (total integration) are used with eight gauss points (referenced as C3D8 inAbaqus code).The computation is divided in four steps: the first step is devoted to the computation of $\tilde{F}^e \approx \tilde{R}^e$ at the gauss points of each meshing element, the second step extrapolates the $\tilde{F}^e$ values at the node of each element, the third step computes the gradient between the nodes, the fourth step inserts the new values of the gradient at the involved Gauss points.

The $\varLambda$ tensor is thencomputed at each Gauss pointas well as the GND densities λ^s on the slip systems (s).
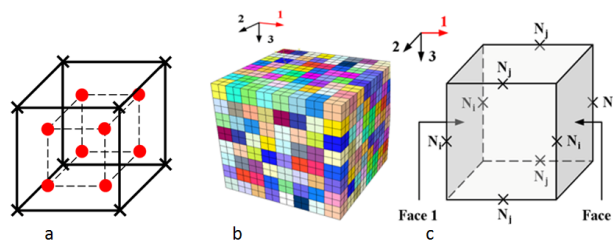

Fig.5. (a) Meshing element (Gauss points are represented by o symbols and the nodes of the elements are represented by X symbols), (b) aggregate used for the identification of the model parameters, (c) boundary conditions.

4.3   Identification of the model parameters

The identification is performed by an inverse method on a "model" aggregate composed of 512 grains presenting the isotropic texture of the 316LN steel, which meshing is composed of 4,096 square elements C3D8. On the base of the tensile tests, the model parameters are determined, via an interface [47, 48] between Sidolo® [64] and Abaqus®. The aggregateused for the identification is given in Fig.5band the boundary conditions (Fig.5c) are supplied in table 2.

Boundary conditions	Face 1	Face2	Nodes Ni, i≠j	Nodes Nj, i≠j
	u1=0	u1=U(t)	u2(Ni)=0	u2(Nj)=0

Table 2.Boundary conditions.

Some parameters(such as elastic constants and the interaction matrix coefficients)have been found in the literature.The studied316LN polycrystal was found to be elastically isotropic. But each grain being considered as a single crystal presentsan anisotropic elasticity. Identification of the parameters isthus performed with anisotropic values. For a 316LN single crystal, we use the anisotropic values obtained by Huntington [65] (C11=198GPa, C12= 125 GPa and C44=122GPa).

For austenitic phase, weuse the interaction matrix proposed by Devincre et al [66]. According to these authors, the a^{su}components depend on the applied strain, via the dislocation density magnitude. In this work,we have used the a^{su}asymptotic values.The matrix is composed of six terms representing several types of dislocation interactions: $a_0$forself interaction, $a_1$forcollinear interactions, $a_2$for Lomer Cottrell locks, $a_3$for Hirthjunctions, $a_4$forglissile dislocation interactions, $a_5$for sessile dislocation interactions. Forα iron,the a^{su} componentswere obtained by dislocation dynamic simulationsby Monnetet al [61]. In this paper, the a_i/a_0ratio given by Monnet[67]ischosen, but$a_0$is deduced from an inverse method.For austenitic steel, the obtained values (a_0=0.1236, a_1=0.6330, a_2=0.1236, a_3=0.0709, a_4=0.1388 and a_5=0.1236)are close to Monnet's ones.

Three identifications are presented: one corresponding to the local approach (LA) ($k_0=0$), performed on the tensile curve corresponding to a grain size of 26µm; the two others, corresponding to non-local approaches (NLA), are performed on the three grain sizes.

The Burgers vector norm value was determined by Robertson et al [68]. For our 316LN, initial total dislocation density ρ_0 is measured by TEM.

The parameters independent of the type of approach are: the b Burgers vector norm, the ρ_0 initial dislocation density, the$\dot{\gamma}_0$ reference shear rate and the rate exponent n. These parameters are given in table3:

b (m)	ρ_0 (m^{-2})	n	$\dot{\gamma}_0$ (s^{-1})
2.5410^{-10}	1.7710^{12}	73.50	4.00 10^{-11}

Table 3. Physical parameters independent of the type of approach

From the identification performed thanks to tensile tests, two sets of (K, k_0 and 2y_c) parameters are found for small and moderate strains. The evolution of these parameters at different stages of the tensile curves could have been determined, but such inverse computation being time consuming, we have reduced our study to the twostrain ranges given in table 4.

In the following, the non-local approach corresponding to small and moderate strains are named NLA1 and NLA2 respectively. The local approach ($k_0=0$) is named LA.

	τ_0 (MPa)	k_0 (-)	K (-)	y_c(m)
LA	22.30	0	59.97	1.29 10^{-9}
NLA1 $\varepsilon \leq 1\%$	22.30	150	88	9.14 10^{-9}
NLA2 $1\% \leq \varepsilon \leq 15\%$	22.30	8.25	47.00	4.45 10^{-9}

Table 4. Material parameters identified from experimental data.

Being an intrinsic value,the friction shear stress τ_0 is taken constant for the three identifications. $2y_c$ is a material parameter related to an annihilation distance of dislocations equal to an amplitude of a few Burgers vectorsb. Table 4 shows that $2y_c$ variationsare ranging from9b to 70b. The material parameter K is related to the dislocation mean free path by Eq.19.For LA, the values of L_G^s are about 48μm. For NLA1 and NLA2, they are 40 μm and 53 μmrespectively.Such values, slightly larger than the grain size, are relevant values for the initial state of an annealed material. According to Acharya and Beaudoin[16], the parameter k_0 is bound to the "mean free path". Its value is 150 for small strains and 8.3 for larger strains. The 316LN steel used in this paper did not present residual stresses, so, the GND initial density is assumed equal to zero.

The identification process gives 3 sets of parameters (K, y_c, k_0) which values depend on the strain amplitude. This means that Eq.23 should take into account this fact. In this first approach, we have successively used the relevant values for each stage of the simulations.

4.4   Validation of the local and non-local approachesthrough tensile curves

In Fig.6a, simulations of the tensile test performed with LA on AG2 aggregate are compared to experimental tests (grain size 26 μm).Fig.6b,c,d shows that the non-local approach NLA2 ($1\% \leq \varepsilon \leq 15\%$), gives a good description of the grain size effect on tensile tests ($\dot{\varepsilon} = 10^{-3} s^{-1}$).The numerical curves fit with experimental ones, except for the micro-plasticity stage. This slight misfit comes from an hardening matrix assumed constant with strain amplitude.
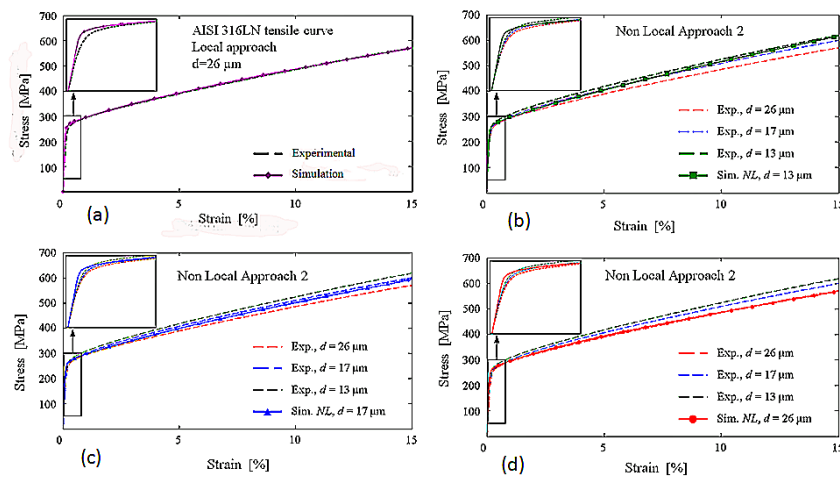

Fig.6. Comparison of experimental and numerical tensile stress-strain curves,(a) Local approach, (b, c, d) Non-local approach ($\dot{\varepsilon} = 10^{-3} s^{-1}$).

For small deformations$(0.3\% \leq \varepsilon \leq 1\%)$, the computed tensile curves obtained with the non-local approach1 (NLA1)fit with the experimental ones (Fig.7a), but as shown in Fig.7b, NLA1 cannot be extended to an applied deformation beyond *1%*.

Thismacroscopicalthreshold strain of 1%,corresponds to an average strain value beyond which all grains are plastically deformed, leading to dislocation patterns.In ourpolycrystal model, the grains are considered as single crystals with different crystalline orientations. The constitutive laws of the model correspond to single crystal laws. The first set of parameters (strain less than 1%) is bound to single crystal stage I (single slip), whereas the second set corresponds to stage II (hardening stage). For polycrystals in micro-plasticity stage, most grains are eitherin elastic stage or in stage I,where the dislocation pattern is not yet developed. At about 1%macroscopical strain, the change on the hardening slope of the tensile curve corresponds to a plastic deformation of all grains and then to hardening.
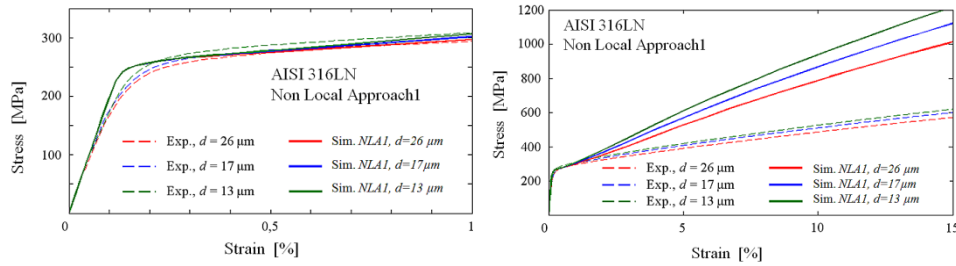
Fig.7. Experimental and numerical tensile stress-strain curves for the Non-local Approach1. (a) Small deformations, (b) Moderate deformations

5. Results: Hall-Petch law andfatigue behaviour

5.1 Grain size effect for monotonic loading

For moderate applied strain (Fig.8a),NLA2 simulations of the Hall-Petch curves,are in very good agreement with experimental curves. Fig.8b shows the predicted hardening slopes for small grain sizes ranging between d=5 µm and d=500 µm. A large hardening is observed for very small grain sizes.
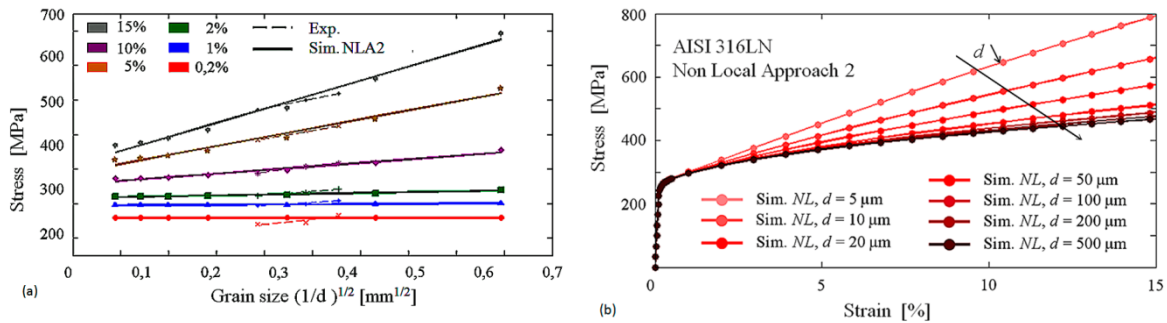

Fig.8. (a) Comparison of experimental and stress-grain size curves simulation. (b) Simulation of the tensile test for polycrystals presenting several small grain sizes with the Non-local Approach2 (NLA2) for k_0=8.25 (moderate straining).

5.2 Fatigue loading

5.2.1 Comparison of Local and Non-local approaches

Computed fatigue curves obtained for 20 cycles $(\varepsilon = \pm 0.5\%)$ with LA and NLA1are compared to an experimental one. As it can be seen on Fig.9, LAidentified from tensile tests does not fit with the fatigue life curve. By contrast, NLA1 gives a good description of the hardening stage of the fatigue curve.Nevertheless, the latter non-local approach cannot describe the whole fatigue curve. This means that the dislocation microstructure evolution towards a two-phase material composed of walls, cells and persistent bands [69,70]cannot be predicted by our model without introducing back stresses.
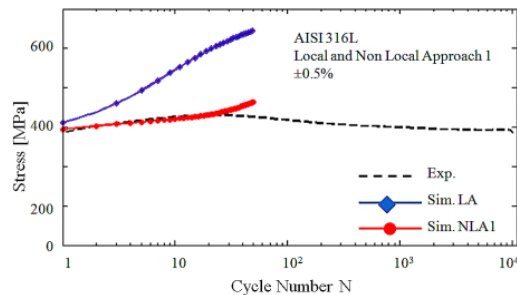

Fig.9. Comparison of the fatigue curves in the hardening stage computed with the Local Approach (LA) and Non-local Appoach 1 (small strain, k_0=150) and the experimental one.
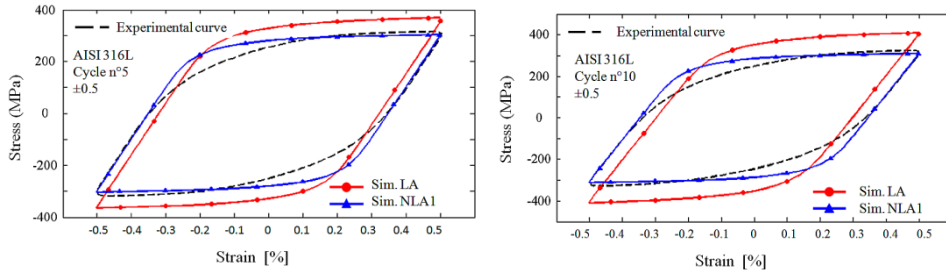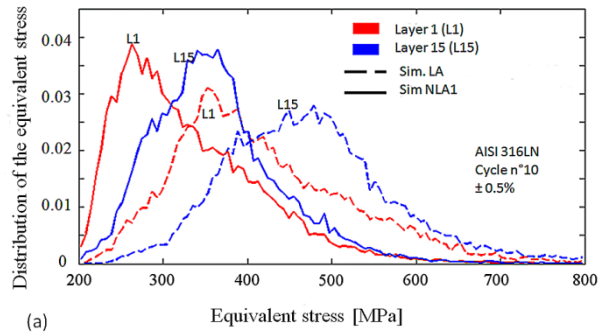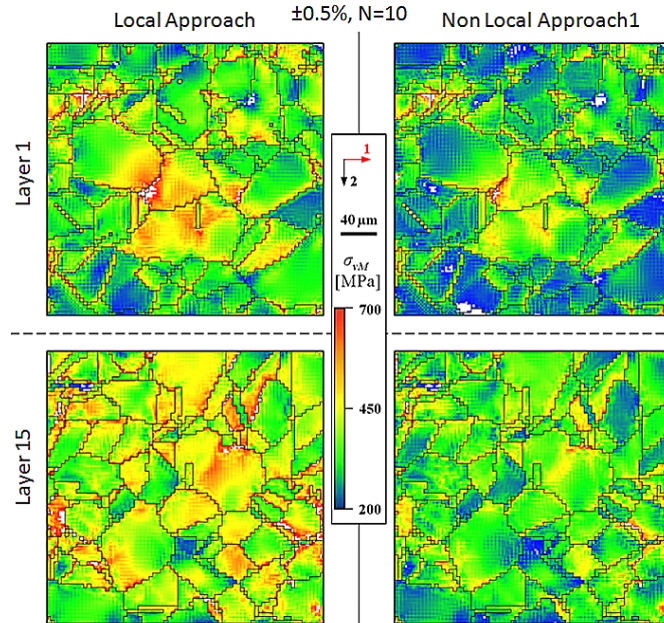
Fig.10. Comparison of the fatigue stress-strain curves in the hardening stage computed with the Local Approach (LA) and Non-local Appoach 1 (small strain, k_0=150) and the experimental one (5th and 10th fatigue cycles).

As shown in Fig.10, the non-local approach gives a better description of the hysteresis loops of the hardening fatigue stage, by comparison with the local approach. Nevertheless, there is a slight discrepancy at the transition between elastic and plastic stages. This discrepancy may be explained by the absence of back stress, generally introduced in the constitutive law (Eq.16) for fatigue description.

NLA mappings, as well as the distribution curves, show that introduction of GNDs densities lower the local equivalent stress values, when compared to LA (Fig.11a and Fig.11b). GNDs relax the internal stresses at grain boundaries but also relax them within the grains. The decrease of the average stress is about 100 MPa.

(a)

(b)

Fig.11. Comparison of the equivalent stress field computed with the Local approach (LA) and the non-localapproach NLA1 corresponding to small strain (k_0=150)and performed on the AG2 aggregate submitted to fatigue test (10th cycle).(a) Distribution curves of the equivalent stress amplitude, (b)mapsof equivalent stress field within the 1st and 15th layers of the aggregate.

The maps (Fig.11) show that the local intragranularstress fields present heterogeneities. The strain fields,not given here, also showheterogeneities. For the polycrystal model, a more accurate threshold might be applied to each Gauss point, but such a refinement would lead to a more complex simulation. Schwartz et al [40] showed that polycrystal model could describe accurately the PSBs pattern at end of the hardening stage. In this paper, the meshing is too large to describe such a pattern.

5.2.2 *Grain size effect in fatigue loading*
Grain size effect in fatigue is studied for AG2 and AG2D10 aggregates after 10 cycles (fatigue hardening stage). At the vicinity of the grain boundaries,the stresses are increased and are less homogeneously distributed in small grain sizeswhen compared to large grain sizes (Fig.12a and Fig.12b).
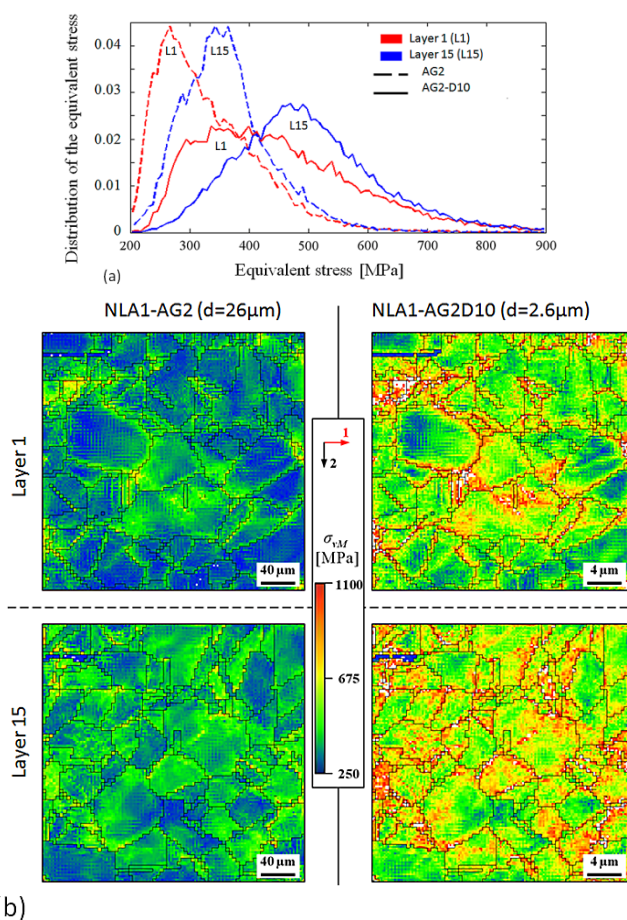

Fig.12. Comparison of the equivalent stress field computed with the Local Approach(LA) and the Non-local Approach 1 corresponding to k_0=150 (NLA1) performed on the 2AG aggregate submitted to fatigue test (10th cycle). (a) Distribution curves of the equivalent stress amplitude, (b) maps of equivalent stress field within the 1st and 15[th]layers of the aggregate.

6. Discussion

A simple non-local model has been designed to predict the hardening stage, the cyclic stress-strain response and the distribution of the internal stress field within the grains of an actual 316LN

aggregatecontaining 1,029 grains. For the macroscopical and microscopical mechanical behaviour of a 316LN steel, the contribution of GNDswhich take into account all local deformation incompatibilities, has been studied by comparing the numerical results of local and non-local models to experimental ones. The GND densities on the slip systems have been introduced in the evolution law of the total dislocation density and into the Schmidcriterion (τ_c). Instead of using 9components on 12 slip systems for the dislocation tensors $\tilde{\alpha}^s$, we have represented the GND densitiesby 12 scalarsλ^s, according toAcharya and Beaudoin [18]. Thus, only one parameter (k_0)has been added to the material parameters of our local polycrystal model.

A set of three material parameters (K, y_c and k_0) is determined throughan inverse method,using experimental tensile tests performed on polycrystals presenting three grain sizes. Two sets of parameters have been obtained for small and moderate straining. The $k_0$parameter bound to GNDs mean free path drops from 150 for small strains *($\varepsilon<1\%$)*to 8 for moderate strains *($1\%<\varepsilon<15\%$)*. For moderate strains, our result is of the same order of magnitude as those obtained byKok et al [71] who found k_0=20.2 for pure nickel (77K and $\varepsilon \geq 5\%$) and k_0= 2.64 for HY-100 martensite.

The existence of two sets of identified parametersfor two different strains raises some open questions. For standardmodeling, K and *$2y_c$* are related respectively to the mean free path of the statistically stored dislocations and to an annihilation distance of dislocations. These two parameters are usually considered as physical parameters, intrinsic to the material. Forthe local approach (LA) and non-localapproach for small and moderate strains (NLA1 and NLA2), K is of the same order of magnitude.By contrast,$2y_c$ presentssome variations: $9b$ for LA, $70b$ for NLA1 and $34b$ for NLA2 (b is the norm of the Burgers vector). Though these data are not clearly defined in literature, the $2y_c$discrepancy istoo large. Last but not the least, the k_0 parameter, is decreased by a factor 20 from the micro-plasticity stage to the hardening stage. In this paper, the used mean free path expression($k_0\lambda^s$) is very close to the one proposed by Kok et al [71]. According to our results, the $k_0\lambda^s$ term of Eq.18(which physical meaning has not yet been clarified)must take into account the evolution of the microstructure (total dislocation densities). In this first numerical approach, we have kept the classical expression of a mean free path but we have separated the case of small and moderate strains.Thefirst k_0 value is obtained from micro-plasticity stage of tensile curve where only few grains are plastically deformed and where the dislocation microstructure is close to the initial one. This value canbe used to describe the cyclic stress strain curves in the hardening stage. The second k_0 value can describe Hall Petch curves for moderate strain but cannot describe fatigue behaviour. It corresponds to a dislocation microstructure different from the fatigue one.This result shows that the expression of the mean free path of GNDs (Eq. 23) is not intrinsic for the material and must be replaced by a function. Eq. 23 is composed of two hardening terms (sources of dislocations) and a recovery term.

In our approach, the hardening and recovery terms are needed to describe the non linear hardening of tensile curves. This recovery term describes the annihilation of two dislocations. However, this term is not suitable to describe a softening due to a different mechanism, such as the motion of dislocations within the channels of the dislocation pattern. Compared to the local approach (without kinematic hardening), the non-local investigation brings a significant improvement on the description of the Bauschinger effect. Nevertheless, it has to be upgraded to completely describe the Bauschinger effect due to the back stress. The back-stress (or kinematic hardening) corresponds to the elastic reaction of the dislocation lattice against the imposed strain at the end of each cycle: glide dislocations are gradually trapped into the loop patches, and into the grain boundaries and PSBs. To avoid the introduction of an empirical non-linear back stress to describe softening, we have to modify the second term of Eq. 23.

This first approach of the hardening in low cycle fatigue provides some important results.In the hardening stage (10th cycle), the NLA1 approach predicts a decrease of the equivalent local stress, when compared to the LA approach. By contrast to the LA mappings, the NLA1 stress pattern mappings show that the equivalent stresses are more concentrated close to the grain boundaries than within the grain bulks.The computing process being time consuming and needing large memory space,

14

the GND densities computed for each time increment are not saved independently, but added to the statistically stored dislocations. To obtain an order of magnitude of the GNDs density ρ_G^s forsmall strain, it is assumedthan the GNDs mean free path is of the same order that the grain size (d=26μm). With $L_G^s = 1/k_0 \lambda^s = d$ and $\lambda^s \approx \left(\rho_G^s\right)^{1/2}$,we obtain: λ^s=2,500 m^{-2} and ρ_G^s =6.2 10^6.m^{-2}. Such a low value of ρ_G^s is relevantfor an annealed material.

A NLA approach givesinformation about the grain size effect in fatigue loading.For two studied grain sizes (d=26μm and d=2.6 μm), computations point out larger stress distribution for small grains (average stress shifted about 150 MPa), meaning a larger non uniform stress pattern and a large concentration of stresses near some grain.
For AG2 aggregate, the meshing (4μm x 4μm x 5μm)used for computation is too large to capture very small lattice misorientations between neighboring points. According to Kadkhodapouret al [52], GNDs measurements related to small misorientationsmust be recorded witha 50nm step size. The obtained local stress and strain field in the real 316LN aggregate can be used to test damage criteria.

7. Summary

To check the validity of the laws, we have numerically tested these equations on tensile and low cycle fatigue loadings.The main advantage of our straightforward non-local approach is to only need seven physical parameters (τ_0, n, a_0, ρ_0, k_0, K and y_c) which can be experimentally identified from tensile tests performed on different grain sizedpolycrystals. When compared to the local approach, the non-localapproach, identified on the micro-plasticity stage of tensile tests, is a very efficient tool to predict the hardening stage of fatigue, cyclic stress-strain curves and the related local stresses. Our results show that a better formulation of the GND mean free path must be investigated to describe the back-stress phenomenon. The proposed non-local approach gives also a first hint of the grain size effect during fatigue.

References
[1] S. Zaefferer, J.-C.Kuo, Z. Zhao, M. Winning, D. Raabe, On the influence of grain boundary misorientation on the plastic deformation of aluminium bicrystals. Acta Mater. 51 (2003) 4719-4735.
[2] A. Ma, F. Roters, D. Raabe, On the consideration of interaction between dislocations and grain boundaries in crystal plasticity finite element modeling theory, experiments and simulation, Acta Mater. 54 (2006) 2181-2194.
[3]D.L. McDowell, Viscoplasticity of heterogeneous metallic materials, Mater.Sci. Eng. R62 (2008) 67-123.
[4] D.L. McDowell, Perspective on trends in multiscale plasticity, Int. J. Plast. 26 (2010)1280-1.
[5] N.A. Fleck, G.M. Muller, M.F. Ashby, J.W. Hutchinson, Strain gradient plasticity; theory and experiment, Acta Metall. Mater. 42 (1994) 475-487.
[6] N.A. Fleck, J.W. Hutchinson, Strain gradient plasticity, Adv. Appl. Mech. 33 (1997) 295-361.
[7] N.A. Fleck, J.W. Hutchinson, A reformulation of strain gradient plasticity, Adv Applied Mechanics. 49 (2001) 2245-2291.
[8] S. Forest, Milieux continus généralisés et matériaux hétérogènes, Transvalor, presses des Mines de Paris 2006.
[9] S. Forest, F. Barbe, G. Cailletaud,Cosseratl of size effects in the mechanical behaviour of polycrystals and multi-phase materials, Int. J. Solids Structures. 37 (2000) 7105-7126.
[10] A. Zeghadi, S. Forest, A.-F.Gourgues, O. Bouaziz, Cosserat continuum modeling of grain size effects in metal polycrystals, Procceding in Applied Mathematics and Mechanics. 5 (2005) 79-82.

[11] N.M. Cordero, A. Gauber, S. Forest, E.P. Busso, F. Gallerneau, S. Kruch, Size effect in generalized continuum crystal plasticity for two-phase laminate, J. Mech. Phys. Solids58 (2010) 1963-1994.

[12] J.F. Nye, Some geometrical relations in dislocated solids.ActaMetall1 (1953) 153-162.

[13] M.F.Ashby, The deformation of plastically non-homogeneous materials, Phil. Mag. 21 (1970) 399-424.

[14] J.D. Eshelby, The determination of the elastic field of an ellipsoidal inclusion and related problems, Proceeding of the Royal Society of London (1957) A 376.

[15] E. Kröner, Konstinuumstheorie der Versetzungen und Eigenspannungen, In Ergebnisse der angewantenMathematik, Springer Verlag, Berlin 1958.

[16] A.J. Beaudoin, P.R. Dawson, K.K. Mathur, U.F. Kocks, A hybrid finite element formulation for polycrystal plasticity with consideration of macrostructural and microstructural linking, Inter. J. Plasticity 11 (1995) 501–521.

[17] A. Acharya, J.L Bassani,Lattice incompatibility and gradient theory of crystal plasticity, J. Mech. Phys. Solids. 48 (2000) 1565-1595.

[18] A. Acharya, A.J. Beaudoin, Grain size effect in viscoplasticpolycrystals at moderate strains, J. Mech. Phys. Solids 48 (2000) 2213-2330.

[19] A. Acharya, J.L. Bassani, A. Beaudoin, Geometrically necessary dislocation hardening, and a simple gradient theory of crystal plasticity, Scripta Mater. 48 (2003) 167-172.

[20] A. Acharya, A. Roy, Size effects and idealized dislocation microstructure at small scales: Prediction of Phenomenological model of Mesoscopic Field Dislocation Mechanics: Part I. J. Mech. Phys. Solids 54 (2006) 1687-1710.

[21] A. Acharya, New inroads in an old subject: plasticity, from around the atomic to the macroscopic scale, J. Mech. Phys. Solids. 58 (2010) 766-778.

[22] F.T. Messonnier, E.P. Busso, N.P. O'Dowd, Finite element implementation of a generalised non-local rate-dependent crystallographic formulation for finite strains, Inter. J. Plast. 17 (2001) 601-640.

[23] D. Raabe, M. Sachtleber, Z. Zhao, F. Rotters, S. Zaefferer, Micromechanical and macromechanical effect in grain scale polycrystal plasticity, experimentation and simulation, Acta Mater. 49 (2001) 3433-3441.

[24] L.P. Evers, W.A.M. Brekelmans, M.G.D. Geers, Scale dependent crystal plasticity framework with density and grain boundary effects, Inter. J. Solids Structures 41 (2004) 5209-5230.

[25] R.J. Asaro, J.R. Rice, Strain localization in ductile single crystals, J. Mech. Phys. Solids 25 (1977) 309-338.

[26] R.J. Asaro, Geometrical effects in the inhomogeneous deformation of ductile single crystals, Acta Metall. 23 (1979) 445-453.

[27] R.J. Asaro, A. Needleman, Texture development and strain hardening in rate dependent polycrystals, ActaMetall 33 (1985) 923-953.

[28] D. Peirce, R.J. Asaro, A. Needleman, An analysis of nonuniform and localized deformation in ductile single crystal, Acta Metall. 30 (1982) 1087-1119.

[29] D. Peirce, R.J. Asaro, A. Needleman, Material rate dependence and localized deformation in crystalline solids, Acta Metall. 31 (1983) 1951-1976.

[30] M.E. Gurtin, 2002. A gradient theory of single-crystals viscoplasticity that account for geometrically necessary dislocations, Int. J. Mech. Solids 50 (2002) 5-32.

[31] M.E. Gurtin, 2003. On framework for small- deformation viscoplasticity: free energy, microforces, strain gradients, Int. J. Plasticity 19 (2003) 47-90.

[32] M.E. Gurtin, L. Anan, The decomposition F=FeFp, material symmetry and plastic irrotationality for solids that are isotropic-viscoplastic or amorphous, Inter. J. Plasticity 21 (2005)1686-1719.

[33] P. Cermelli, M.E. Gurtin, On the characterization of geometrically necessary dislocations in finite plasticity, J. Mech. Phys. Solids 49 (2001)1539-1568.

[34] A. Beaudoin, A. Acharya, S. Chen, D. Korzekwa, M. Stout, Consideration of grain-size effect and kinetics in the plastic deformation of metal polycrystals, Acta Mater. 48 (2000) 3409-3423.

[35] E.P. Busso, F.T. Meissonnier, N.P. O'Dowd, 2000. Gradient-dependent deformation of two-phase single crystals, J. Mech. Phys Solids 48 2333-2361.

[36] J.C. Mach, A.J. Beaudoin, A. Acharya, Continuity in the plastic strain rate and its influence on texture evolution, J. Mech. Phys Solids 58 (2010) 105-128.

[37] J.L. Chaboche, A review of some plasticity and viscoplasticity constitutive theories, Inter J Plast. 24 (2008) 1642–1693.

[38] L. Taleb G. Cailletaud, An updated version of the multimechanism model for cyclic plasticity, Inter. J. Plast. 26 (2010) 859-874.

[39] K. Said, Multi-mechanism models: Present state and future trends, Int. J. Plast.27 (2011) 250-281.

[40] J. Schwartz, O. Fandeur, C. Rey, fatigue initiation modeling of 316LN steel based on Nonlocal plasticity, Journal of ASTM International, Vol7, (2010) 7 paper IDJAI102552.

[41] A. Le Pécheur, F. Curtit, M. Clavel, J.M. Stephan, C. Rey, P. Bompard, Polycrystal modelling of fatigue: Pre-hardening and surface roughness effects on damage initiation for 304L stainless steel, Int. J. Fatigue 45 (2012) 48-60.

[42] Y. Li, V. Aubin, C. Rey, P. Bompard, Polycrystalline numerical simulation of variable amplitude loading effects on cyclic plasticity and microcrack initiation in austenitic steel 304L, Int. J. Fatigue 42 (2012) 71-81.

[43] H. Mughrabi, Dislocation wall and cell structure and long range internal stresses in deformed metals crystals, Acta Mater. 31 (1983) 1367-1379.

[44] Armstrong, Frederick. A mathematical representation of multiaxialbaushinger effect.CEGB Report RD/B/N731, Berkeley, Nuclear laboratories (1966).

[45] C. Déprés, M. Fivel, L. Tabourot, A dislocation-based model for low amplitude fatigue behaviour of faced-centred cubic single crystals, Scripta Mater. 58 (2008) 1086-1089.

[46] P. Erieau, C. Rey, Modelling of deformation and rotation bands and of deformation induced grain boundaries in IF steel aggregate during large plane strain compression, Inter. J. Plasticity 20 (2004) 1763-1788.

[47] M. Libert, L. Vincent, B. Marini, C. Rey, Temperature dependant polycrystal model. Application to bainitic steel under tria-xial loading in the ductile brittle transition, Inter. J. Sol. Struct. 48 (2011) 2196-2208.

[48] D. Cédat, O. Fandeur, C. Rey, D. Raabe, Polycrystal model of the mechanical behavior of a Mo-TiC30vol.% metal-ceramic composite using a 3D microstructure map obtained by a dual beam FIB-SEM, Acta Mater. 60 (2012) 1623-1632.

[49] J. Schwartz, Approche non-locale en plasticité cristalline: application à l'étude du comportement mécanique de l'acier AISI 316 LN en traction simple et en fatigue oligocyclique, Thèse de Doctorat, Ecole Centrale Paris 2011.

[50] B.P. Kashyap, K. Tangry, On Hall-Petch relationship and substructural evolution in type 316L stainless steel, Acta Metall. Mater. 43 (1995) 3971-3981.

[51] A. Needleman, J.GilSevillano, Preface to the viewpoint set on: geometrically necessary dislocations and size dependent plasticity, Scripta Mater 48 (2003) 109-111.

[52] J. Kadkhodapour, S. Schmauder, D. Raabe, S. Ziaei-Rad, U. Weber, M. Calcagnotto, Experimental and numerical study on geometrically necessary dislocations and non-homogeneous mechanical properties of ferrite phase in dual phase steel, Acta Mater 59 (2001) 4387-4394.

[53] L. Tabourot, M. Fivel, E. Rauch, Generalised constitutive laws for FCC single crystals, Mat. Sci. Eng. A, (1997) 234-236 639-642.

[54] U.F. Kocks, A.S. Argon and M.F. Ashby, Thermodynamics and Kinetics of slip progress in Materials Science 19, Pergamon Press Oxford 1975.

[55] U.F. Kocks, Laws for work hardening and low-temperature creep, J. Eng. Mater. Tech. 98 (1976) 76-85.

[56] Y. Estrin, H. Mecking, A unified phenomenological description of work hardening and creep based on one-parameter models, Acta Metall. 32 (1984) 57-70.

[57] Y. Estrin, H. Mecking, Microstructural aspect of constitutive modeling of plastic deformation, Elastic-plastic failure modelings of structures with applications, D. Hui and T.J. Kozikeds, vol 141 181-191. ASME, New York 1988.

[58]E.Schmid, Proc. Int. Conf. Applied Mechanics (1924), p.342, Delft.

[59] B. Devincre, L. Kubin, T. Hoc, Physical analyses of crystal plasticity by DD simulation, Scripta Mater. 54 (2006) 741-746.

[60] S. Queyreau, G. Monnet, B. Devincre,Slip systems interaction in s-iron determined by dislocation dynamics simulations, Int J. Plasticity 25 2 (2009) 174-181.

[61] G. Monnet, C. Domain, S. Queyreau, B. Devincre, Atomic and dislocation dynamics simulations of plastic deformation in reactor pressure vessel steel, J. Nuclear Material 394 (2009) 174-181.

[62] C. Teodosiu, J.L. Raphanel, L. Tabourot, Finite element simulation of the large elastoplastic deformation of multicrystals. MECAMAT'91, Teodosiu, Raphanel&Sidoroff (eds) © Balkema, Rotterdam, 1993 153-160.

[63] S. Zaefferer, S.I. Wright, D. Raabe, Three-Dimensional Microscopy in Focused Ion Beam-Scattering Electron Microscope: A New Dimension of Microstructure Characterization, Mater. Trans. A 39A (2008) 374-389.

[64] G. Cailletaud, P. Pilvin, Identification and inverse problems related to material behaviour. Proceedings of the International Seminar on Inverse problems, Clamart, 1994 79-86.

[65] H.B. Huntington, The elastic constants of crystals, Solid State Physics (1958) 214-351.

[66] B. Devincre, L. Kubin, T. Hoc, Dislocation mean free paths and strain hardening of crystals, Science 320 (2008) 1745-1748.

[67] G. Monnet, A crystalline plasticity law for austenitic stainless steel, Note interne EDF 2009.

[68] C. Robertson, M.C Fivel. , A. Fissolo, Dislocation substructure in 316L stainless steel under thermal fatigue up to 850 K, Mater. Sci. Eng. A315 (2001) 47-57.

[69] H. Mughrabi, On the current understanding of strain gradient plasticity, Materials Science and Engineering 387 (2004) 209-213.

[70] H. Mughrabi, Dual role of deformation-induced geometrically necessary dislocations with respect to lattice plane misorientations and/or long range internal stresses, Acta Mater. 54 (2006) 3417-3427.

[71] S. Kok, A.J. Beaudoin, D.A.Tortorelli, On the development of stage IV hardening using a model based on the mechanical threshold, Acta mater 50 (2001) 1653-1667.